Canadian Mineralogist
Vol. 20, pp. 393-410 (1982)

EQUILIBRIUM IN Mn–Fe–Mg ALUMINOUS PELITIC COMPOSITIONS AND THE EQUILIBRIUM GROWTH OF GARNET

TIMOTHY P. LOOMIS AND FRANCIS B. NIMICK*
Department of Geosciences, University of Arizona, Tucson, Arizona 85721, U.S.A.

ABSTRACT

Thermodynamic data were adopted from published sources and derived from two natural assemblages for the Mg, Fe, and Mn end-members of garnet, biotite, chlorite and cordierite, and for other major phases found in aluminum-silicate-saturated pelitic assemblages. These data represent a simplified model system that is self-consistent and can be used to calculate compositions of exchange phases that are similar to those observed in natural assemblage, whereas the interior of the garnet remains Fe system destroys the "loop" character of equilibrium between two phases on T–X diagrams and renders phase compositions dependent on the bulk composition. The model thermodynamic system was used to simulate the growth of garnet in equilibrium with chlorite. Chlorite is thought to be the primary source of the Mn that becomes concentrated in garnet. The "equilibrium growth simulations" assume that equilibrium is maintained between the garnet edge and the entire matrix assemblage, whereas the interior of the garnet remains chemically isolated. The simulated profiles show excellent agreement with the generally observed profile morphology in natural samples and predict reasonable phase compositions. The simulations predict that the temperature of the first appearance of tiny grains of Mn-rich garnet is highly sensitive to the bulk MnO content of the rock, but that the major explosive growth of Fe-rich garnet that marks the almandine isograd is relatively independent of MnO content. Consequently, the tiny grains of Mn-rich garnet may be overlooked in rocks at metamorphic temperatures below that of the obvious almandine isograd. Increasing pressure and Fe/Mg ratio in the bulk composition should increase the amount of garnet grown in equilibrium with chlorite. Discontinuities of zoning profiles and periods of garnet resorption interspersed with growth are shown to be possible results of equilibrium growth in response to normal, prograde metamorphism.

Keywords: phase equilibrium, crystal growth, garnet, computer simulation.

SOMMAIRE

On évalue les données thermodynamiques de la littérature ou dérivées d'assemblages naturels pour les pôles Mg, Fe et Mn des phases grenat, biotite, chlorite, cordiérite et autres minéraux importants des roches pélitiques saturées en silicate d'aluminium. Ces données représentent un système modèle simplifié et cohérent qui peut servir à calculer, pour les phases en relation d'échange, une composition rappelant celle des roches naturelles. L'addition de Mn au système binaire Mg–Fe détruit le caractère en boucle de l'équilibre entre deux phases sur coupes T–X, et fait dépendre ces compositions de phase de la composition globale de la roche. Le modèle thermodynamique sert à simuler la croissance du grenat en équilibre avec la chlorite, source probable du Mn qui se concentre dans le grenat. Ces "simulations de croissance à l'équilibre" supposent l'équilibre maintenu entre la bordure du grenat et l'assemblage total de la matrice, tandis que le noyau du grenat reste chimiquement isolé. La forme des profils simulés concorde avec celle des profils observés et conduit à prédire des compositions de phases satisfaisantes. La température à laquelle apparaissent les premiers petits cristaux de grenat manganifère est très sensible à la teneur de la roche en MnO, mais la croissance soudaine et importante de grenat ferrifère qui marque l'isograde de l'almandin est quasi-indépendante de cette teneur. A cause de leur taille minuscule, ces cristaux de grenat manganifère pourraient facilement passer inaperçus dans les roches dont la température de métamorphisme est inférieure à celle de l'isograde de l'almandin. Une augmentation de la pression et du rapport Fe/Mg dans la composition globale devrait accroître la production du grenat en équilibre avec la chlorite. Les discontinuités dans le profil de zonation et l'alternance des périodes de résorption et de croissance du grenat résulteraient tout simplement de la croissance à l'équilibre que provoque le métamorphisme prograde normal.

(Traduit par la Rédaction)

Mots-clés: équilibre des phases, croissance cristalline, grenat, simulation par ordinateur.

INTRODUCTION

Since the electron microprobe became a tool

*Present address: Sandia Laboratories, Albuquerque, New Mexico 87185, U.S.A.

used by petrologists, compositional zoning has been reported in garnet from almost every geological environment, including eclogites, volcanic flows, fumaroles, skarns, granites and contact and regional metamorphic rocks. It is the zoning in garnet in metamorphosed pelitic rocks, however, that displays the most regular pattern and is amenable to simulation by computer. Simulations of the prograde growth of garnet in pelitic rocks are presented in this and the following paper (Loomis 1982) to (1) investigate the processes by which crystals grow and (2) consider the accuracy with which garnet zoning records the history of conditions imposed on metamorphic rocks.

Many investigators have recorded what have come to be regarded as "typical" characteristics of zoning in garnet in pelitic rocks: Mn decreases symmetrically outward and is compensated for primarily by a rise in Fe; Mg is very low in the core and increases slightly outward (*e.g.*, Harte & Henley 1966, Crawford 1966, Brown 1967, Atherton 1968, Hollister 1969, Edmunds & Atherton 1971, Okrusch 1971, Banno & Kurata 1972, Jones 1972, Black 1973, Korikovskiy *et al.* 1974, Arkai *et al.* 1975, Yardley 1977, Woodsworth 1977 and Fletcher & Greenwood 1979). Ca zoning is much less regular, although one distinctive pattern has been linked to the presence of epidote coexisting with garnet (*e.g.*, Banno & Kurata 1972, McAteer 1976); in our simulations, we assume that the grossularite content of garnet is constant. The success of our simulations is judged by comparison of Mn, Fe and Mg zoning profiles with the generalized pattern described above.

In metapelitic rocks containing high-temperature assemblages, garnet zoning is slight or nonexistent (*e.g.*, Blackburn 1969, Gable & Sims 1969, Dallmeyer & Dodd 1971, Hess 1971, Okrusch 1971, Loomis 1972, Henry 1974, Ashworth 1975, Harris 1976, Keys & Medaris 1976, Schmid & Wood 1976, Seidel *et al.* 1976, Tracy *et al.* 1976, Yardley 1977, Woodsworth 1977, Fletcher & Greenwood 1979, Stephenson 1979), probably owing to the efficacy of diffusion at high temperatures. The simulations reported here were computed at low to moderate temperatures, so that diffusion may be assumed to have negligible effects on compositional profiles during the growth process.

A number of thermodynamic and phase-assemblage assumptions were adopted to achieve tractable simulations. These assumptions are sufficiently important to warrant a description in the following sections.

The Source of Mn

One of the most distinctive features of compositional zoning in garnet in metapelitic rocks is the bell-shaped profile for Mn. It is well known that this profile is generated by fractionation because Mn is partitioned strongly into garnet relative to coexisting phases (*e.g.*, Hollister 1966). The accurate simulation of Mn zoning in garnet is especially sensitive to the representation of partitioning between garnet and phases that are the major sources of Mn during the early stages of garnet development. Phases found in pelitic rocks at grades below garnet stability that can contain significant amounts of Mn are chloritoid, carbonates, muscovite, ilmenite and chlorite. Although any one of these minerals may be the important Mn-bearing phase in a given rock, only the most common situation is desired for simulation.

Chloritoid can contain the highest concentration of Mn of any of the minerals listed above, but it is restricted to rocks of special composition and cannot be the common Mn-bearing phase in low-grade rocks. Carbonate minerals may also have a significant concentration of Mn, but these minerals usually occur only in trace amounts in pelites, and thus are excluded as a possible source for the Mn in garnet. Muscovite at low grades has a significant phengitic (Fe^{2+} + Mg + Mn) component. Sekino *et al.* (1973) described muscovite from a pegmatite in which Mn/(Mn + Al^{VI} + Fe) approaches 0.025. But muscovite in most regional metamorphic rocks contains a concentration of Mn that is too small to be significant in garnet formation.

Ilmenite is a common accessory phase in metapelitic rocks and may contain up to 30 wt. % MnO (Czamanske & Mihálik 1972). Yet there is evidence to suggest that rutile or anatase (or both) are the stable Ti-bearing minerals found in sediments and low-grade metamorphic rocks (Pettijohn 1949, Frey 1978, McCallister *et al.* 1978, Fletcher & Greenwood 1979). Neither of these minerals contains significant concentrations of MnO. Therefore, although ilmenite can participate in higher-grade garnet-forming reactions, we assume that it is not the most common phase to contribute Mn to garnet.

Numerous data support the role of chlorite as the major Mn-bearing phase at low grades of metamorphism. Firstly, the only major phases in pelitic rocks at temperatures near

300°C are chlorite, white mica, and quartz (Weaver & Beck 1971). Of these, only chlorite can contain significant Mn. Kurata & Banno (1974) have shown a roughly linear relationship between increasing Mn in garnet and decreasing Mn in chlorite with increasing grade of metamorphism. In addition, many of the garnet-forming reactions proposed in the literature involve chlorite as a reactant (see Winkler 1974). For these reasons, and because of the paucity of thermodynamic data for most phases stable under low-grade conditions, we have chosen to simulate the growth of garnet by consumption of manganous chlorite at a low grade of metamorphism in this work. Simulations of the development of garnet by simultaneous consumption of both chlorite and biotite will be presented in a future paper.

Model Thermodynamic System

Pelitic rocks in metamorphic environments equilibrate under a wide range of pressures and temperatures, ranging from 300 to 800°C and from 2 to 20 kbar. The equilibrium assemblage also depends on the initial bulk-composition and on the influences of transport processes on the chemical potential of mobile components. Owing to a paucity of data, however, several assumptions are necessary in order to develop a tractable but useful model system.

Table 1 lists the phases used in the model system, together with their constituent oxides. All are phases commonly found in rocks of pelitic composition. There are additional phases that are not included, most notably chloritoid, staurolite, amphibole and pyroxene. Natural chloritoid and staurolite are found only in rocks of restricted compositions (Hoschek 1967), and few thermodynamic data exist. Pyroxene occurs only in granulite-facies rocks, which form at pressure–temperature conditions outside the range considered. Amphibole, in addition to being restricted to bulk compositions enriched in alkalis, has solid-solution properties that are intractable at the present time.

Model assemblages are assumed to be saturated in the following compositional units: either muscovite or K-feldspar, quartz, and pyrophyllite or an aluminum silicate phase. $P(H_2O)$ is assumed to be a large fraction of total pressure. Pelitic rocks commonly contain graphite, and it has been suggested (*cf.*, Ganguly 1977) that in the temperature range 300–600°C, water constitutes approximately 50 to 80% of the vapor phase. Quartz and either muscovite or a

TABLE 1. THERMODYNAMIC DATA

Mineral	Formula	ΔH_f°	S°	a	b	c	d	V°
Quartz	SiO_2	-217650	9.88	11.22	.00820	-270000	-	.5422
Water	H_2O	-57796	45.10	7.30	.0025	-	-	-
Muscovite	$KAl_3Si_3O_{10}(OH)_2$	-1427408	68.80	97.56	.0264	-2544000	-	3.3630
K-feldspar	$KAlSi_3O_8$	-949188	51.13	76.62	.0043	-2994500	-	2.6020
Pyrophyllite	$Al_2Si_4O_{10}(OH)_2$	-1345313	57.20	79.43	.0392	-1728200	-	3.0258
Andalusite	Al_2SiO_5	-615866	22.20	41.31	.0063	-1239210		1.2316
Kyanite	Al_2SiO_5	-616897	20.00	41.39	.0068	-1288210	-	1.0538
Sillimanite	Al_2SiO_5	-615099	23.13	40.02	.0074	-1167410		1.1926
Pyrope	$1/3Mg_3Al_2Si_3O_{12}$	-499721	21.21	63.93	-.0076	-187380	-580	.9012
Almandine	$1/3Fe_3Al_2Si_3O_{12}$	-419512	25.20	32.52	.0112	-624333	-	.9184
Spessartine	$1/3Mn_3Al_2Si_3O_{12}$	-449367	24.80	31.49	.0111	-637300	-	.9393
Phlogopite	$1/3KMg_3AlSi_3O_{10}(OH)_2$	-496022	25.37	33.54	.0096	-716667	-	1.1923
Annite	$1/3KFe_3AlSi_3O_{10}(OH)_2$	-410732	31.70	35.48	.0099	-643667	-	1.2294
Manganophyllite	$1/3KMn_3AlSi_3O_{10}(OH)_2$	-434778	31.45	34.47	.0098	-656667	-	1.2586
Clinochlore	$1/5Mg_5Al_2Si_3O_{10}(OH)_8$	-424340	21.30	32.56	.0101	-817600	-	1.0110
Daphnite	$1/5Fe_5Al_2Si_3O_{10}(OH)_8$	-338675	27.78	34.51	.0105	-744600	-	1.0574
Mn Chlorite	$1/5Mn_5Al_2Si_3O_{10}(OH)_8$	-363732	27.53	33.49	.0103	-757600	-	1.0866
Mg - Cordierite	$1/2\ Mg_2Al_4Si_5O_{18}\cdot H_2O$	-1128919	55.72	77.62	.0129	-1930000	-	2.8826
Fe - Cordierite	$1/2\ Fe_2Al_4Si_5O_{18}\cdot H_2O$	-1040880	63.80	79.56	.0132	-1857000	-	2.9006
Mn - Cordierite	$1/2\ Mn_2Al_4Si_5O_{18}\cdot H_2O$	-1067749	63.55	78.55	.0131	-1870000	-	2.9298

° denotes 298.15 K and 1 bar. ΔH_f°: enthalpy of formation from the elements (cal/mole); S°: entropy (cal/mole K); a, b, c, d: coefficients in the heat capacity equation $C_p = a + bT + cT^{-2} + dT^{-1/2}$, where T is absolute temperature (cal/mole K, cal/mole K^2, cal K/mole, cal/mole $K^{1/2}$ respectively); V°: molar volume (cal/bar).

K-feldspar are commonly present in pelitic compositions. The most restrictive assumption is that only pelitic compositions sufficiently rich in Al to maintain aluminum silicate phases are considered here.

The philosophy applied in this work is to use simple thermodynamic models to extrapolate equilibria by a small amount from conditions where they are defined by natural assemblages, rather than to attempt a prediction of realistic assemblages from basic data using complex models, both of which are scarce for metamorphic minerals. Consequently, ideal solution of Mg, Fe and Mn end-members, normalized to formulae with one exchangeable cation, is assumed. Mn commonly comprises over 10% of the exchange sites in metamorphic garnet and should not be treated as a trace element.

Derivation of thermodynamic data

Many of the thermodynamic data were adopted from Helgeson *et al.* (1978) as a self-consistent set. Values of water fugacity are interpolated from data given by Burnham *et al.* (1969). Other thermodynamic data were estimated or calculated from partitioning of elements in natural assemblages as described below.

Values for standard-state (298.15 K and 1 bar pressure) entropy ($S°$), volume and heat-capacity coefficients were estimated for Mn-chlorite, manganophyllite, Fe-cordierite and Mn-cordierite from substitution equations. For example, from the substitution equation Mg-cordierite + FeO = Fe-cordierite + MgO, the value of $S°$ of Fe-cordierite can be estimated as $S°$ (Fe-cordierite) = $S°$ (Mg-cordierite) + $S°$(FeO) − $S°$(MgO). $S°$ for pyrope was adopted from Haselton & Westrum (1979), standard-state volume from Robie *et al.* (1978), and heat-capacity coefficients from Newton *et al.* (1977). All other data are taken from Helgeson *et al.* (1978).

The standard-state enthalpy of formation from the elements ($\Delta H°_f$) of spessartine was estimated using the method of Chen (1975) and the following series of constituent reactions:

$$3\,MnO + Al_2O_3 + 3\,SiO_2$$
$$3\,MnO + Al_2SiO_5 + 2\,SiO_2$$
$$3\,MnSiO_3 + Al_2O_3$$
$$\tfrac{3}{2}\,Mn_2SiO_4 + Al_2O_3 + \tfrac{3}{2}\,SiO_2$$
$$\tfrac{3}{2}\,Mn_2SiO_4 + Al_2SiO_5 + \tfrac{1}{2}\,SiO_2.$$

Data for the phases listed were taken from Helgeson *et al.* (1978) and Robie *et al.* (1978). The estimated value for $\Delta H°_f$ fo spessartine is −449,367 cal/mol. The method was tested by deriving $\Delta H°_f$ for almandine by the same process, yielding an estimate within 0.008% of the value derived below and within 0.1% of the value derived using data of Ferry & Spear (1978). Consequently, we believe that the above estimate for $\Delta H°_f$ of spessartine is sufficiently accurate for our purposes. The $\Delta H°_f$ of clinochlore, daphnite, pyrope, almandine, manganophyllite and Mn-chlorite were derived from observed partitioning in natural assemblages as follows.

The basic assemblage used was CV204 reported by Ghent (1975): garnet–biotite–chlorite–staurolite–kyanite–muscovite–quartz–plagioclase–ilmenite. This assemblage was chosen, rather than assemblages from lower grades reported by others, because the temperature and pressure of equilibration were established by several methods, there is no evidence of disequilibrium, and an aluminum silicate is present. Partitioning of Mg and Fe among the phases in CV204 is typical of the assemblage measured. The equilibration temperature of the assemblages was assumed to be 813 K, and $P(H_2O)$ was assumed to be 4 kbar. These estimates are consistent with the constraints suggested by Ghent (1975). The total pressure was assumed to be 5 kbar, probably a minimum value for these rocks. The greater amount of Mn in assemblage Gh117 (without kyanite) allowed the partitioning of Mn to be measured more accurately, and these partitioning data were applied to assemblage CV204 to estimate complete compositions of phases with sufficient precision to derive the thermodynamic data for the Mn end-members. The compositional data used are reported in Table 2.

The following Fe end-member reaction between biotite and garnet is shown as an example of the method used to derive $\Delta H°_f$ of almandine:

$$K_{1/3}FeAl_{1/3}SiO_{10/3}(OH)_{2/3} + \tfrac{2}{3}Al_2SiO_5 + \tfrac{1}{3}SiO_2 \rightleftharpoons$$
$$FeAl_{2/3}SiO_4 + \tfrac{1}{3}\,KAl_3Si_3O_{10}(OH)_2. \qquad (1)$$

Using an expression of the form $C_p = a + bT + c/T^2 + d/T^{1/2}$ for heat capacity, the free energy of reaction (ΔG^*_r) at the temperature (T) and pressure (P) of interest is calculated as

$$\Delta G^*_r = \Delta H^\circ_r - T\Delta S^\circ_r + \Delta a_r\,(T - T^\circ - T\ln(T/T^\circ)) - \tfrac{1}{2}\Delta b_r(T - T^\circ)^2 - \tfrac{1}{2}\Delta c_r[(T - T^\circ)^2/T^{\circ 2}T] + 2\Delta d_r\,(2T^{1/2} - T^{\circ 1/2} - T/T^{\circ 1/2}) + (P - P^\circ)\Delta V^\circ\,(\text{solids}) + n(H_2O)RT\ln[f(H_2O)^*] \qquad (2)$$

TABLE 2. MOLE FRACTIONS OF END MEMBERS IN PHASES USED TO DERIVE THERMODYNAMIC DATA

Source	End Member	Garnet	Biotite	Chlorite	Cordierite
Ghent (1975)	Fe	.7105	.3732	.3025	
	Mg	.1184	.4690	.4530	
	Mn	.0263	.0004	.0006	
	Other	.1448	.1574	.2439	
Okrusch (1971)	Fe	.7713	.5153		.5191
	Mg	.0789	.2588		.4633
	Mn	.1151	.0036		.0166
	Other	.0347	.2223		.0010

where T° and P° are standard-state temperature and pressure, ΔH°_r and ΔS°_r are enthalpy and entropy of reaction at standard-state conditions, $\triangle a_r$, $\triangle b_r$, $\triangle c_r$, and $\triangle d_r$, are the differences of heat-capacity coefficients for reaction, $n(H_2O)$ is the number of moles of water involved in the reaction, and $f(H_2O)$* is the fugacity of water at T and P. Where garnet and biotite are mixtures, the following relationship between phase compositions must be satisfied at equilibrium:

$$\ln \frac{X^G_{Alm}}{X^B_{Ann}} = - \Delta G^*_r/RT, \quad (3)$$

where X^j_i is the mole fraction of end member i (almandine or annite) in phase j, and R is the gas constant. The equations above implicitly assume ideal solution, that $f(H_2O)$ (P°, T) is unity, that $\triangle V^\circ$ approximates the volume change of solids at any pressure, and that the activities of all nonexchange phases are unity.

Adopting the data for annite and other phases from Helgeson *et al.* (1978), $\triangle H^\circ_f$ of almandine is found to be –419,512 cal/mal. The analogous Mg and Mn end-member reactions were used with the data estimated above to derive $\triangle H^\circ_f$ for pyrope and for manganophyllite. Similar reactions between biotite and chlorite were used to derive $\triangle H^\circ_f$ for clinochlore and daphnite; the reaction between garnet and chlorite gives $\triangle H^\circ_f$ for Mn-chlorite.

The $\triangle H^\circ_f$ data for cordierite were estimated using average partitioning data reported by Okrusch (1971) for several samples with the assemblage garnet–biotite–cordierite–sillimanite–quartz–plagioclase–K-feldspar. Because his tabulated data represent average compositions of garnet, the edge composition, assumed to be the equilibrium one, was first estimated from zoning data presented by Okrusch. Then the temperature of equilibration was calculated using equation (3), the analogous Mg end-member reaction, and the thermodynamic data adopted above. The calculated temperatures were within 2 K of each other, and an equilibrium temperature of 934 K was assumed for the following calculations. The pressure was assumed to be 2.5 kbar and $P(H_2O)$ equal to total pressure. In order to make the phase composition of garnet agree *exactly* with the assumed thermodynamic data, temperature and pressure, it was necessary to modify slightly the original estimate of garnet to produce the composition listed in Table 2; it is emphasized that the small change to the garnet composition is well within the analytical uncertainty of measurement. Equations analogous to (1) for reaction between biotite and cordierite were used to derive $\triangle H^\circ_f$ for the three end-members of cordierite.

The result of these calculations is a set of thermodynamic data consistent with most of the data presented by Helgeson *et al.* (1978) and with the two natural assemblages presented in Table 2. These data represent an internally consistent *model system* suitable for our purposes; they are not meant to compete in accuracy with data derived from geothermometric calculations using more sophisticated solution-models. The data will continually change as more experimental data become available and determination of the conditions of formation of natural assemblages improves. Inaccuracies in the solution model will probably cause the calculated compositions of the phases to be increasingly less accurate as their compositions deviate more and more from those of the natural samples. The small extrapolations considered here for the chlorite–garnet assemblage and the comparability of simulations and natural assemblages suggest that the simulations are not grossly inaccurate. At any rate, the sense of variation of compositions is believed to be meaningful.

Calculation of stable assemblages

The composition of two phases that can exchange two components at equilibrium can be illustrated on a T–X phase diagram, as shown for the model system in Figure 1A. Similar diagrams have been derived by thermodynamic and empirical methods (*e.g.*, Thompson 1976). For an arbitrary number of components, we require for each phase j that

$$\sum_i X^j_i = 1 - X^j_a, \quad (4)$$

where X^j_i is the mole fraction of component i in phase j and where X_a represents the mole fraction of additional cations held constant. For the binary case, the two equations (4) plus the two equations (3), one for each end-member reaction, yield a simple, unique analytical solution

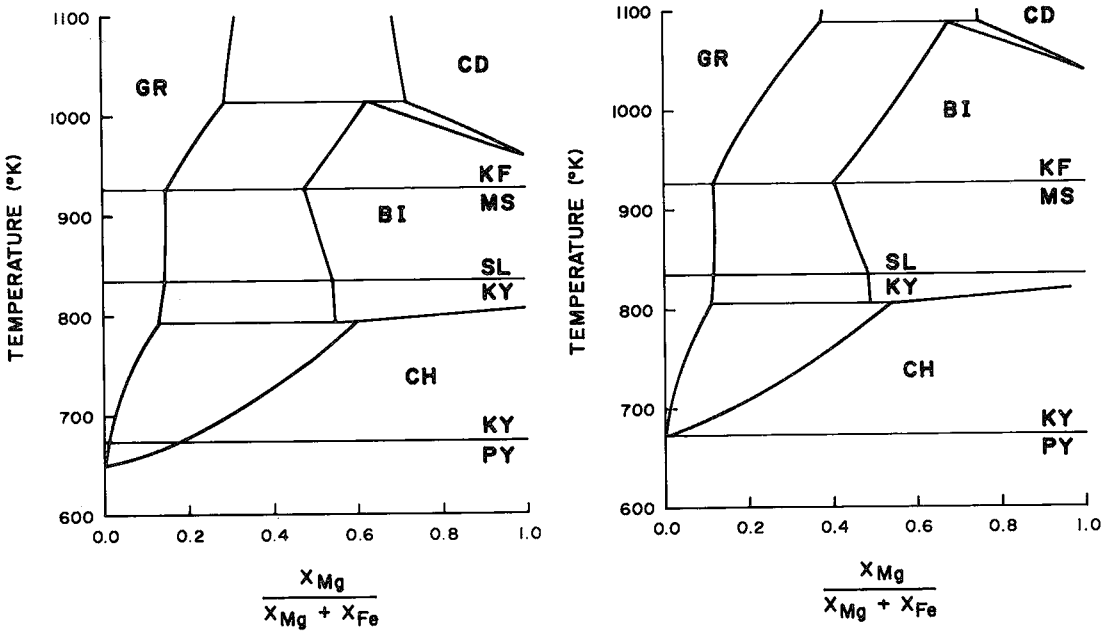

FIG. 1. Calculated phase-diagrams for pelitic assemblages saturated with quartz, K-feldspar or muscovite, and aluminum silicate or pyrophyllite at 5 kbar total pressure and 4 kbar water pressure. Fields where only one exchange-phase is stable are labeled: GR garnet, CH chlorite, BI biotite, CD cordierite, Two exchange-phases coexist in the regions between labeled fields (the chlorite – biotite loop plots as a single line). Compositionally independent reactions are shown as horizontal lines; PY pyrophyllite, KY kyanite, SL sillimanite, MS muscovite and KF K-feldspar. A (on left). The exchange phases contain only Fe and Mg end-members. B (on right). The exchange phases contain a constant mole fraction of end-member components (additional cations) other than Fe and Mg in the amount: garnet 0.1, biotite 0.18, chlorite 0.24, cordierite nil.

for the phase compositions. The abundance of each phase can then be determined from the material-balance equations, one for each component i,

$$\sum_j X_i^j M_j = A_i \qquad (5)$$

where M_j is the molar abundance of phase j and A_i is the total molar abundance of component i in the assemblage. The equilibrium compositions calculated for coexisting phases plot as loops in T–X space.

Multiple loops can be calculated at each temperature, one for each possible pair of exchange phases. In the binary system, the stable loops at each temperature can be identified by the criteria: (1) the mole fractions of components in all phases are positive (*i.e.*, the loop exists on the diagram) and (2) either the garnet composition is the most Fe-rich or the cordierite composition is the most Mg-rich. The success of this method is based on the fact that the composition of co-existing exchange-phases is independent of the bulk composition. Therefore, all loops at each temperature can be calculated regardless of the bulk composition, and the phase compositions can be compared to determine which loops are stable. The stable assemblage for the bulk composition is determined by comparing the ratio Mg/(Mg + Fe) of the bulk composition with the ranges occupied by the stable two-exchange-phase loops and one-exchange-phase fields.

The calculation of phase compositions of two exchange phases at equilibrium in the ternary system Fe–Mg–Mn is also accomplished by solving the set of 9 constraints given by equation (3) for each end-member reaction, equation (4), and equation (5). We used an analytical (quadratic) solution to this set of equations and chose the solution, if any, that gave positive mole fractions of components in all phases.

The calculation of the stable assemblage in the Fe–Mg–Mn ternary system is complicated by the fact that the phase compositions depend upon

the bulk composition of the system. If the bulk composition lies outside a two-exchange-phase loop (actually a surface in 3-component space), the calculated phase-compositions are different from those for bulk compositions within the loop (phase compositions also vary with the bulk composition within the loop). Consequently, it is not possible to simply compare phase compositions to determine which assemblages are stable in the ternary system. The stable assemblage was identified by its minimum free-energy for the specific bulk-composition in question as follows.

Phase abundances were calculated from the molar balance requirements that all the Mn, Mg and Fe be accommodated within the two exchange-phases (eq. 5). Assemblages yielding negative abundances were rejected. The abundance of the additional phases muscovite or K-feldspar, aluminum silicate or pyrophyllite, quartz and water, were calculated to consume the remaining equilibrating bulk-composition. The free energy of the assemblage was calculated by summing the free-energy contribution of the Mn, Mg and Fe end-member components in the exchange phases and the free energy of the additional phases.

The free energy of possible one-exchange-phase assemblages was calculated in a similar way, with the simplification that the composition of the exchange phase could be determined directly from the bulk composition and equation (4). The assemblage yielding the minimum free-energy was assumed to be stable. A practical consideration is that the free-energy differences among several possible assemblages can be on the order of 0.001% or less, if reaction temperatures are to be determined within 1°C. Thus, it is necessary to specify reaction coefficients and thermodynamic data to at least 10 significant digits and to use double precision arithmetic on most computers.

Calculated Phase-Diagrams and Partitioning

Binary phase-diagram

The calculated phase-diagram for aluminum-silicate-saturated assemblages at 5 kbar total pressure and 4 kbar water pressure is shown in Figure 1. Figure 1A shows the phase stabilities calculated assuming that all exchange phases are binary solid-solutions of Mg and Fe only. Figure 1B shows the corresponding diagram, where each exchange-phase contains a constant mole fraction of elements other than Mg and Fe ("additional cations") in the amount: garnet 0.1, biotite 0.18, chlorite 0.24, and cordierite none. The second case (additional cations) corresponds most closely to the natural data from which critical thermodynamic data were derived. Consequently, the compositions of phases used in the simulations include constant amounts of additional cations as listed above; the phase diagram in Figure 1B shows the appropriate phase-stabilities for the Mn-free system at 5 kbar pressure.

The effect of additional cations on the relative stabilities of exchange phases shown in Figure 1 illustrates the well-known rule that addition of a component to a system increases the stability field of the phase that incorporates the greater amount of the added component. Thus, the effects of amounts of additional cations other than assumed in these simulations can be estimated from Figure 1. Moreover, it is apparent that Mn will greatly expand the field of garnet stability in Mg–Fe projection.

Comparison with natural assemblages

The phase relations shown in Figure 1 correlate well with assemblages observed in nature, with two major exceptions. The first is the limitation that more than two exchange-phases cannot coexist over a range of temperature. However, since the growth of most of the garnet occurs over the temperature range at which chlorite is the principal source of material, and since biotite and chlorite have very similar compositions when biotite first becomes stable (Fox 1975, Ferry 1976), this limitation is not believed to have a severe effect upon calculated zoning profiles in garnet. Preliminary simulations in the systems where garnet, biotite and chlorite coexist support this conclusion.

The second discrepancy between nature and the calculated phase-diagrams is the relative sequence of phases as temperature increases. The classical Barrovian sequence requires the successive appearance of chlorite, biotite and garnet. Yet the sequence predicted here is chlorite, garnet and biotite. There are a number of possible explanations for this difference. Firstly, rocks having lower Al_2O_3 or higher K_2O than required by our model system and not saturated in aluminum silicate generate biotite before garnet. A second possibility is that biotite is stabilized at lower temperatures by a component that is not considered in the model system, although our examination of other cations did not reveal likely candidates. Thirdly, equilibrium may not be maintained in nature, so that the garnet-forming reaction may be overstepped to

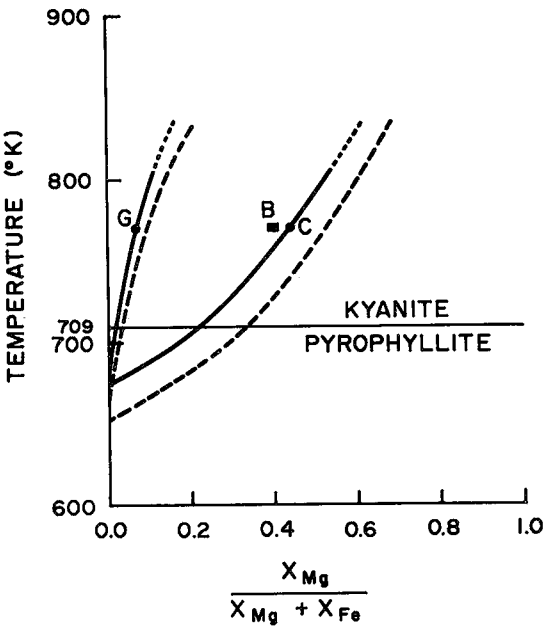

FIG. 2. Phase diagram of the garnet–chlorite assemblage at 5 kbar total pressure and 4 kbar water pressure. Garnet contains 0.1 and chlorite 0.24 mole fraction of cations in addition to Fe, Mg and Mn. Solid curve: Fe–Mg binary (dotted where metastable). G and C represent compositions of garnet and chlorite, respectively, that are predicted to be in equilibrium at 775.6 K for a bulk composition such as B. Dashed curve: pseudobinary loop in which the mole fractions of Mn in chlorite and garnet are fixed at their equilibrium values for the bulk composition in Table 3 at the lowest temperature at which garnet is stable; C_1 and G_1 as defined in Figure 3. Dotted where metastable.

sufficiently high temperature that biotite forms from chlorite before garnet appears. A fourth possibility is that tiny nuclei of garnet do form before biotite, but that they are seldom observed. This possibility will be discussed below.

In summary, we believe that the model system developed here can serve to usefully approximate equilibrium processes in aluminous pelitic compositions.

TABLE 3. BULK COMPOSITION USED IN SIMULATIONS

Component	SiO_2	$AlO_{1.5}$	FeO	MgO	MnO	$KO_{.5}$
Wt. Percent	58.47	22.11	7.60	2.84	.05	5.24
Mole Fraction	.5521	.2461	.0600	.0400	.0004	.0631

The effect of Mn on garnet – chlorite equilibrium

Two fundamental difficulties in presenting graphically the predictions of the thermodynamic model for a three-component system are: (1) the content of each of the three components in a phase changes with temperature and pressure, and (2) phase compositions depend on the bulk composition of the system. Before introducing unfamiliar representations of composition, we will use Figure 2 to illustrate approximately the effect of Mn on the garnet–chlorite equilibrium. The binary Fe-Mg equilibrium loop is shown by the solid lines in Figure 2 (dotted at temperatures above the loop's stability according to Figure 1B); this is the same loop as shown in Figure 1B. The equivalent dashed loop, shown for comparison, was computed in the following way. The compositions of garnet and chlorite were determined for the typical aluminous pelitic bulk-composition listed in Table 3 at the tem-

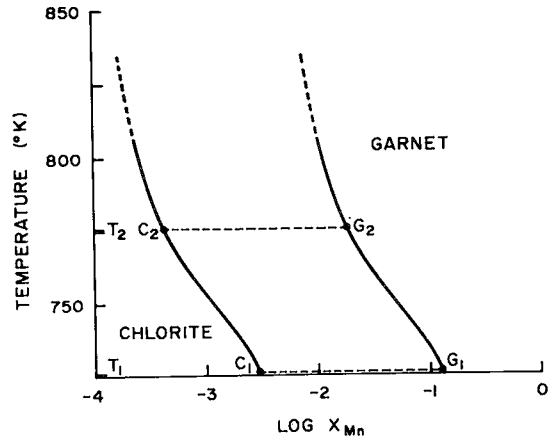

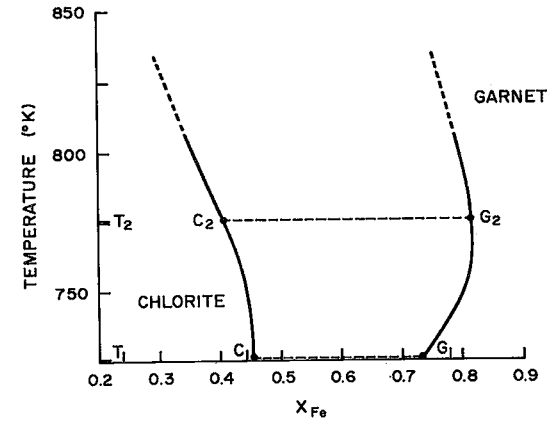

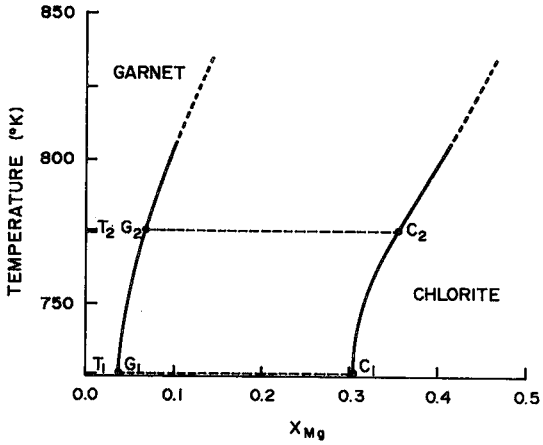

FIG. 3. Phase diagrams of the garnet–chlorite assemblage at 5 kbar total pressure and 4 kbar water pressure for the bulk composition of Table 3 (without fractionation of the bulk composition by garnet). Dashed where metastable. C_1 and G_1 show the compositions of chlorite and garnet, respectively, at the lowest temperature that garnet is stable (725.6 K). C_2 and G_2 show the equilibrium compositions at 775.6 K, representing 50 K overstepping of garnet nucleation. Abscissae: X_{Mn} (Fig. 3A), X_{Fe} (Fig. 3B), X_{Mg} (Fig. 3C).

perature at which garnet first became stable with rising temperature (725.6 K). The mole fractions of Mn in garnet and chlorite were held constant at these values to calculate the dashed loop.

Comparison of the two loops in Figure 2 illustrates the profound effect on garnet stability of the addition of a small amount of Mn. Mn greatly reduces the temperature at which garnet becomes stable. Because an ideal solution model was used, the calculated effect of Mn on the garnet–chlorite equilibrium is due simply to the concentration of Mn in garnet relative to chlorite, rather than to any nonideal interaction of Mn, Fe and Mg in the phases.

Accurate representations of calculated equilibrium-compositions of phases at 5 kbar total pressure, 4 kbar water pressure, and the bulk composition of Table 3 are shown in Figures 3A–C. They can be used to determine the equilibrium composition of phases when garnet first starts to grow, but after garnet has formed, fractionation of the matrix bulk-composition will affect the equilibrium compositions because they are a function of bulk composition in the ternary system. G_1 and C_1 show the compositions of garnet and chlorite, respectively, when garnet first becomes stable with increasing temperature (the phase diagram cannot be calculated for a lower temperature). G_2 and C_2 show the equilibrium compositions of garnet and chlorite if garnet begins to develop only after 50 K overstepping, but is in equilibrium with chlorite for the bulk composition, as discussed in the companion paper (Loomis 1982).

Equilibrium partitioning of Mn

The relative temperature of nucleation of garnet grains has been inferred in the literature from the distribution of Mn between garnet and matrix phases. The assumption is that an elemental partitioning coefficient defined as

$$K_E(\mathrm{Mn}) = \frac{X^G_{Mn}}{X^C_{Mn}}$$

tends toward one with increasing temperature. Whereas this assumption may be true at very high temperatures, the value of $K_E(\mathrm{Mn})$, calculated from the end-member reaction $MnAl_{2/5}Si_{3/5}O_2(OH)_{8/5} + 2/15\ Al_2SiO_5 + 4/15\ SiO_2 = MnAl_{2/3}SiO_4 + 4/5\ H_2O$, increases with temperature over the geological range of temperature examined, as do $K_E(\mathrm{Fe})$ and $K_E(\mathrm{Mg})$. Thus, the use to K_E as a relative geothermometer must be based rigorously on thermodynamic data. It was found, however, that the distribution coefficient defined as

$$K_D^{\mathrm{Mn\text{-}Fe}} = \frac{X^G_{Mn}\, X^C_{Fe}}{X^C_{Mn}\, X^G_{Fe}}$$

for the exchange of Mn and Fe between chlorite and garnet, $MnAl_{2/5}Si_{3/5}O_2(OH)_{8/5} + FeAl_{2/3}SiO_4 = FeAl_{2/5}Si_{3/5}O_2(OH)_{8/5} + MnAl_{2/3}SiO_4$, does change toward one with increasing temperature.

EQUILIBRIUM-GROWTH MODEL

The simplest model of garnet growth that can generate the commonly observed compositional zoning is here called equilibrium growth. The model assumes that the edge of each garnet crystal is in equilibrium with matrix phases and that all matrix phases are in complete equilibrium thoughout the system. It is further assumed that there is no diffusion within garnet, and that the interior of each garnet crystal is isolated chemically from the matrix; thus, the equilibrating matrix composition is fractionated as garnet grows. The model is essentially that of Rayleigh fractionation (Hollister 1966), differing only in the assumptions and calculations

governing partitioning of components between the garnet edge and the matrix.

The total pressure, the water pressure and the number of garnet nuclei are assumed to be constant throughout the simulation. We have used a nucleation density of about 56/cm³ in these simulations (1000 nuclei for the composition of Table 3), an intermediate value for pelitic rocks according to the data of Jones & Galwey (1964), Galwey & Jones (1966) and Kretz (1966, 1973). We do not believe that sufficient data exist at present to attempt realistic simulations including progressive nucleation. Whereas the relationships between growth, temperature and *radius* depend on the assumed nucleation history, the *total volume* reported is independent of nucleation and represents the volume of garnet in one mole of oxides (approximately 18 cm³ of anhydrous rock).

The standard bulk composition used to illustrate growth of garnet is reported in Table 3. This composition represents a typical, Al-rich pelitic rock. The bulk composition used in the simulation is apportioned among the following compositional units: Mg, Fe and Mn end-members of exchange phases, muscovite or K-feldspar, aluminum silicate phases or pyrophyllite, quartz and water. Thus, the bulk composition used in the simulation (Si, Al, ferrous Fe, Mg, Mn, K and H) represents a subset of the complete bulk-composition; other elements and an *additional* amount of the foregoing elements may be incorporated in minor phases and in the end members of exchange phases represented by "additional cations".

Simulations are computed by the following procedure: (1) the compositions and abundances of garnet and chlorite are calculated for the given pressure, temperature and equilibrating (matrix) bulk-composition; (2) if garnet is stable, its molar abundance and composition are used to calculate the corresponding volume; the volume of garnet is distributed equally among all nuclei as a growth shell, and a new radius for the resulting sphere of garnet is calculated; (3) the amount of each component in the garnet grown is subtracted from the equilibrating bulk composition; (4) the new abundance of other phases in the equilibrating bulk-composition may be calculated if desired, and (5) the temperature is increased. It was found necessary to use a secant convergence procedure to find each new temperature during the beginning stage of garnet growth because very small steps in temperature were necessary to limit the radial increment of growth on nuclei.

Equilibrium-Growth Simulations

General growth-history

The first appearance of garnet in the bulk composition of Table 3 can be determined directly from Figures 3A–C, where it is shown as G_1. After fractionation of the bulk composition begins, Figures 3A–C are no longer appropriate, but the progressive development of garnet at the expense of chlorite can be visualized by reference to Figure 2. As the temperature of chlorite with a ratio Mg/(Mg + Fe) of 0.4 is raised, it enters the garnet–chlorite loop (dashed lines) at 725.6 K. The first garnet to form is rich in Mn, and its removal from the bulk composition causes the loop to migrate rapidly toward the Mn-free loop (solid lines). Consequently, only a small amount of garnet is grown until about 760 K, because the stability loop migrates upward along with the rock temperature. After Mn in the chlorite is depleted at about 760 K, however, the loop becomes fixed as shown by the Mn-free loop in Figure 2 (solid), and garnet grows rapidly with increasing temperature. Thus, the early growth-history is controlled by the pronounced effect of Mn on garnet stability, and the later history is controlled by the more subtle influence of Mg–Fe partitioning.

The later growth-history of garnet can be deduced directly from the phase diagram (Fig. 1B) because most of the Mn has been incorporated in garnet and removed from the equilibrating bulk-composition. As garnet grows in equilibrium with chlorite, the equilibrating bulk-composition migrates up the composition curve of chlorite. At 5 kbar, garnet should stop growing at about 806 K, where the garnet–chlorite equilibrium is cut off by biotite equilibria; at this point the equilibrating bulk-composition is predicted to enter the biotite (–kyanite) field.

The overall reaction responsible for garnet growth in the garnet – chlorite assemblage is chlorite + $\frac{2}{15}$ kyanite + $\frac{4}{15}$ quartz = garnet + $\frac{4}{5}$ water. Between the beginning of garnet growth and 806 K, where growth in equilibrium with chlorite should stop, the simulation predicts a reduction of chlorite, kyanite and quartz of 30, 65 and 4 mole%, respectively, for the bulk composition of Table 3.

Garnet is predicted not to resume growth until about 1000 K, when the equilibrating bulk-composition enters the stable garnet–biotite loop, and a single pulse of growth is predicted to occur at about 1090 K when the equilibrating bulk-

composition enters the garnet–cordierite loop. Note that the second stage of growth should begin with a discontinuity in the garnet profile, and the third stage should show rapid growth at a constant composition. It is probable that resorption of garnet would be expected between 806 and 1000 K (biotite field) and again above 1090 K in the cordierite field. Diffusional relaxation of zoning profiles is also probable at higher temperatures. Of course, staurolite and chloritoid equilibria, variations of $P(H_2O)$, variations of "additional cations", and partial melting can affect these predictions.

The following simulations are restricted to growth of garnet in equilibrium with chlorite for the following reasons: (1) most of the Mn zoning in garnet is generated during early stages of growth; (2) the compositional differences that can be used to distinguish between equilibrium and disequilibrium growth-processes are most distinct when garnet first forms, and (3) many uncertainties affect the accuracy of predictions of growth at higher grades. The simulations were computed for the temperature range extending from the first appearance of garnet to 835 K; the metastable portion of the predictions, according to Figure 1, are dashed in the following figures.

Thermal growth-history in the garnet-chlorite system

The effects of bulk composition on the amount of garnet grown at 5 kbar with rising temperature are illustrated in Figures 4 and 5. The volume history for the typical pelitic composition of Table 3 is shown in Figure 4 (curve 1) along with curves for the same composition with 0, 2 and 3 times the amount of MnO. The curve for the Mn-free system corresponds to the growth history of garnet prescribed by the garnet–chlorite loop shown in Figure 1B. The temperature of first appearance of the Fe-rich garnet (*ca.* 757 K) represents the "almandine isograd" for this bulk composition.

The addition of very small amounts of MnO to the bulk composition is seen to have a dramatic effect on the first appearance of garnet,

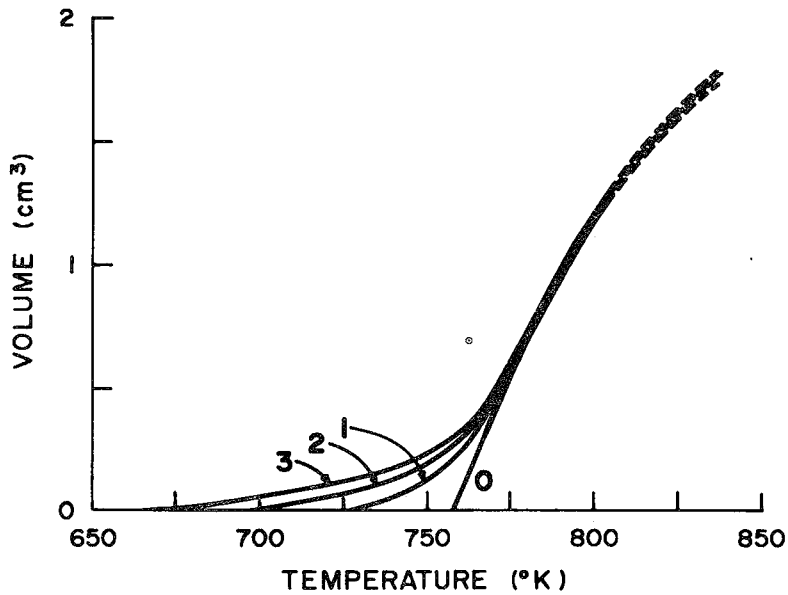

FIG. 4. Total volume of garnet predicted to have crystallized by equilibrium growth in the garnet–chlorite assemblage as a function of temperature (dashed where the garnet–chlorite assemblage is metastable). The total pressure is 5 kbar and the water pressure 4 kbar. Curve 1 was computed for the bulk composition of Table 3 (0.0004 moles MnO). Curves 0, 2 and 3 were computed for the same composition but with zero, 2 and 3 times the amount of MnO. Approximate volume % of garnet in the rock can be obtained by dividing the volume by 18 cm^3/mole.

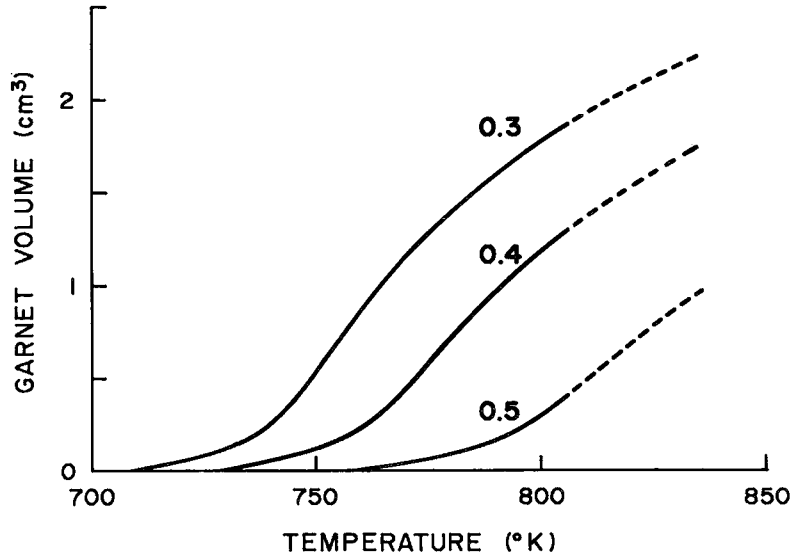

FIG. 5. Total volume of garnet predicted to have crystallized by equilibrium growth in the garnet–chlorite assemblage as a function of temperature (dashed where the assemblage is metastable). Curve 0.4 was computed for the bulk composition of Table 3, having a ratio MgO/(MgO + FeO) of 0.4. Curves 0.3 and 0.5 were computed for the same composition and total MgO + FeO but with the ratio MgO/(MgO + FeO) changed to the labeled value. Approximate volume % of garnet can be obtained by dividing by 18 cm³/mole.

lowering the garnet-isograd temperature over 30 K in response to the MnO content in the typical composition. Even though the first appearance of garnet is stabilized to low temperature by Mn, Figure 4 shows that only a small amount of garnet (about 2½ volume %) is grown before the Mn is depleted and the growth curve for all compositions merge. Moreover, the rate of garnet growth increases rapidly when the "almandine-isograd" temperature of growth of Mn-free garnet is reached. Consequently, the tiny grains of Mn-rich garnet that are predicted to appear at low temperature may be overlooked in contrast to the explosive growth of garnet near the almandine-isograd temperature.

The ratio Mg/(Mg + ferrous Fe) also has a dramatic effect on the garnet-isograd temperature, as can be predicted for the Mn-free system from Figure 1. Thermal growth-histories for garnet in the typical bulk-composition [Mg/(Mg + Fe) = 0.4] and for this composition but with modification of the Mg/(Mg + Fe) ratio (Mg + Fe constant) are shown in Figure 5.

Total pressure has only a small effect on the location of the garnet–chlorite loop and should have little direct effect on garnet growth in this system. Indirectly, however, pressure could have a significant effect by influencing the abundance of "additional cations" and by controlling equilibria that restrict the stability range of garnet–chlorite.

Zoning profiles

The zoning profile simulated for equilibrium growth of garnet from the typical aluminous pelitic composition (Table 3) at 5 kbar pressure is shown in Figures 6–8. As mentioned above, changing the density of nuclei will change the radius of profiles plotted on Figures 6–8, but the compositional history will be unaffected (*i.e.*, the profiles will expand or contract in radius). The first part of the zoning profile is dominated by fractionation of Mn to create the classical bell-shaped spessartine profile. The MnO in the bulk composition is essentially consumed entirely by this process. Because K_E(Mn) is of the same magnitude or greater for other exchange phases (*e.g.*, biotite), the shape of the computed profile for Mn in garnet is substantially the same regardless of assemblage.

Mn exchanges principally with Fe in garnet and chlorite according to the thermodynamic

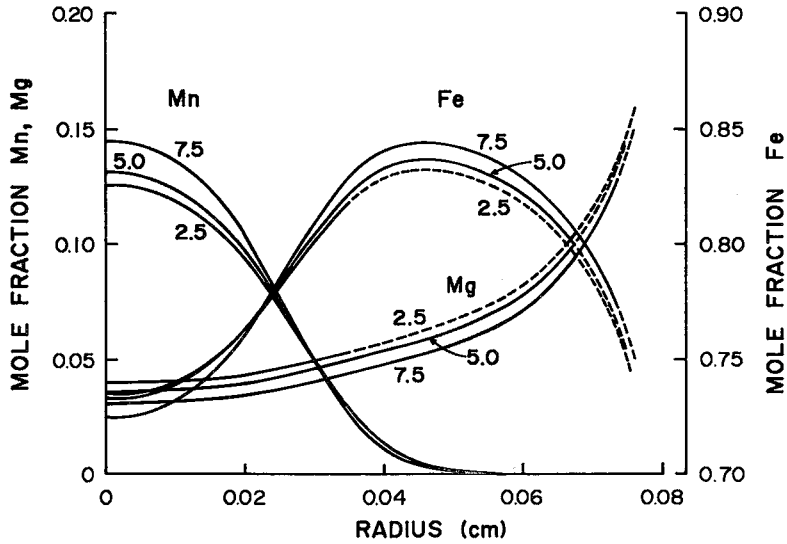

FIG. 6. Simulated profiles of zoning in garnet for equilibrium growth in the assemblage garnet–chlorite at the indicated total pressures (kbar) for the bulk composition of Table 3. The water pressures (bars) are 1600 at 2.5 kbar, 4000 at 5 kbar and 6400 at 7.5 kbar. The curves are dashed where the garnet–chlorite assemblage is predicted to be metastable. Note that the composition axes have equivalent scaling increments.

data, as demonstrated by the computed profiles of zoning. Thus the Fe profile rises rapidly with growth to replace the depleted Mn. After exhaustion of Mn, the zoning profiles of Fe and Mg are controlled by the binary equilibrium loop presented in Figures 1B or 2. In the chlorite–garnet system, both phases become more Mg-rich with increasing temperature, and the Fe profile in Figures 6–8 reflects this requirement. The downturn in the Fe profile would not be as pronounced if garnet were replacing other phases, such as biotite, where phase compositions are less influenced by temperature.

Figure 6 shows that large changes of pressure have very little effect on the zoning profiles, in agreement with Saxena (1969) and Kepezhinskas (1973). Increasing pressure does increase Fe slightly, mainly at the expense of Mn, as predicted from observations of natural rocks by Miyashiro & Shido (1973). An effect that is not seen is an increased content of Mg with increasing pressure, which has been predicted by Green & Ringwood (1968) and other investigators. Increasing pressure does increase the amount of garnet grown in equilibrium with chlorite, as shown by the solid lines in Figure 6. Garnet grown at higher pressure should have a more complete profile of zoning.

Bulk Mn does have a great effect on zoning profiles, as shown in Figure 7. The important observations are: (1) Mn replaces primarily Fe in the garnet core as bulk Mn increases (Mg is only slightly affected); (2) all zoning curves become indistinguisable at a radius greater than about 0.05 cm because the equilibrating Mn has been depleted.

Figure 8 shows profiles for three different values of the ratio Mg/(Mg + Fe) in bulk compositions, otherwise identical with the typical composition of Table 3. It should be noted that this ratio, and thus the zonation in garnet, is a function of the oxidation state of the rock and of the amount of Ti in the bulk composition of the total rock. Chinner (1960, 1962) has studied the effect of oxidation state of iron on the stability of garnet in natural rocks. As expected, the bulk Mg/(Mg + Fe) ratio has a significant effect on the Fe and Mg content of garnet. However, it has essentially no effect on Mn zoning in these simulations because K_E(Mn) is nearly independent of temperature, and ideal solution is assumed. If a nonideal solution model were used, some small effect on Mn zoning could be induced by change of the Mg and Fe contents.

CONCLUSIONS

The simulated garnet-zoning profiles show ex-

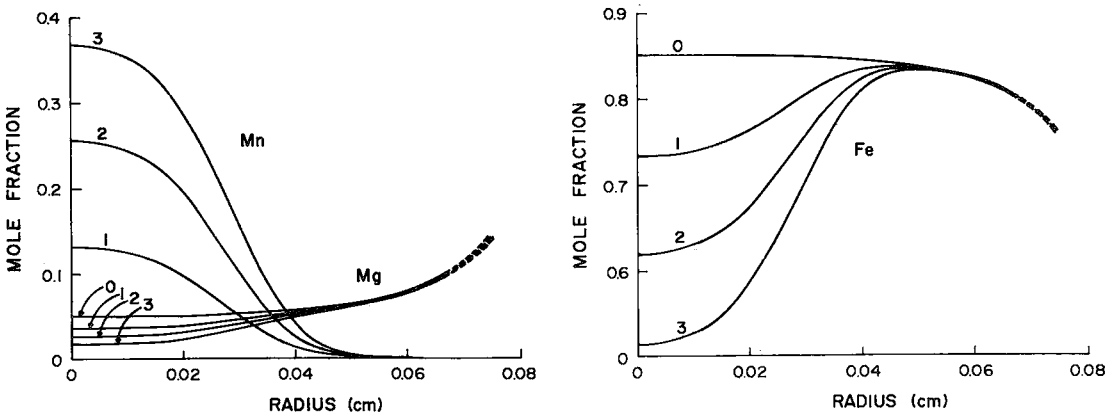

FIG. 7. Simulated profiles of zoning in garnet for equilibrium growth at 5 kbar total pressure and 4 kbar water pressure in the garnet–chlorite assemblage (dashed where metastable) for the bulk compositions described in Figure 4 (labeled multiples of 0.0004 moles MnO). A. Profiles of Mg and Mn. B. Profile of Fe.

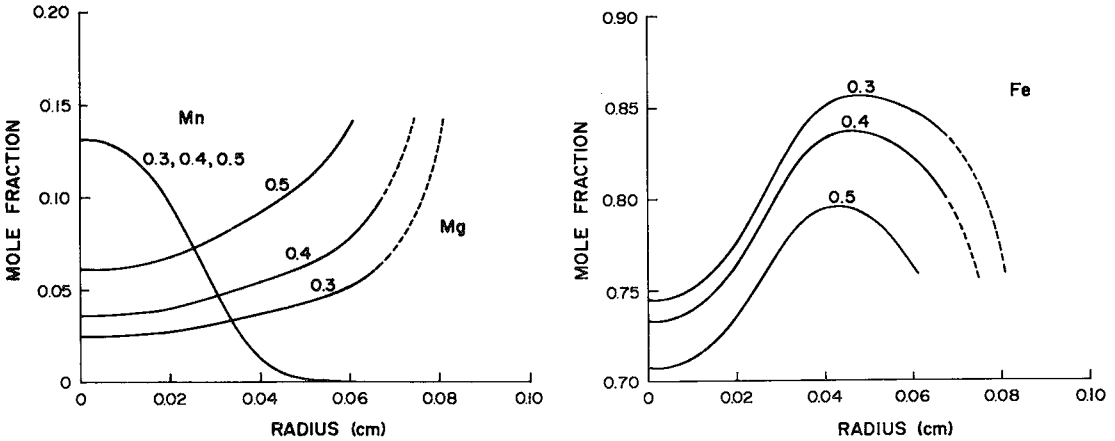

FIG. 8. Simulated profiles of zoning in garnet for equilibrium growth at 5 kbar in the garnet–chlorite assemblage (dashed where metastable) for bulk compositions with the indicated ratios MgO/(MgO + FeO); see Figure 5. A. Profiles of Mg and Mn. B. Profile of Fe.

cellent agreement with the general features observed in prograde growth profiles reported in the literature. The general thermodynamic constraints of (1) fractionation of Mn into the garnet, (2) principal exchange of Fe for Mn, and (3) the gradual enrichment of garnet and chlorite in Mg with increasing temperature combine to produce the typical profile. In view of the importance of bulk composition and nucleation factors, it is remarkable that even the predicted core-composition of garnet and predicted width of the bell-shaped profile are similar to those observed in some natural profiles (*e.g.*, Hollister 1966, 1969). We conclude that the model thermodynamic system used to calculate these profiles, despite the simplification, embodies relationships similar to the ones that govern equilibrium in natural systems. Whereas there is general agreement between simulated equilibrium profiles and observed profiles, the following paper emphasizes variations with grade and composition that point toward the operation of disequilibrium processes in medium-grade metamorphic rocks.

The major source of the Mn that contributes to the high Mn content of garnet in pelitic rocks at the beginning of growth is probably chlorite. Chlorite is the only common mineral

in pelitic rocks that contains sufficient Mn and is sufficiently abundant to supply the required Mn. The first appearance at equilibrium of garnet in the model system is highly sensitive to MnO and Mg/(Mg + Fe) ratio in the equilibrating bulk composition. Even though the small amounts of MnO found in typical pelitic compositions can stabilize the appearance of garnet on the order of 30 K below its appearance in Mn-free compositions, the volume of garnet developed at first is very small. The major onset of garnet growth occurs at the approximate temperature of the "almandine isograd", where Mn-free garnet becomes stable regardless of the MnO content of the bulk composition. Thus, the tiny grains of garnet predicted by the simulations to occur below the obvious "almandine isograd" mapped by most observers could be overlooked. Some support for this suggestion comes from the literature, where a number of investigators have mentioned garnet as an accessory phase that exists below the biotite isograd, even though the garnet isograd had not been reached (Clark 1961, Navarro & Blackburn 1974, de Béthune 1976). Also, in environments in which spessartine garnet forms a major phase, such as in coticules, the grains tend to be very small (*e.g.*, Kramm 1976). Thus, it is quite possible that tiny grains of spessartine-rich garnet may be more common in low-grade rocks than is generally believed.

The total amount of garnet grown in equilibrium with chlorite decreases markedly with increasing Mg/(Mg + Fe) ratio in the bulk compositions. Whereas the amount increases with bulk MnO, the increase is very small. The amount of garnet grown and the completeness of the zoning profile that develops in equilibrium with chlorite increase with pressure.

The phase diagrams of Figure 1 and the simulations illustrate the following facts: (1) a change of assemblage during equilibrium growth of garnet can induce a discontinuity of slope in the zoning profile but not a discontinuity in composition; (2) a hiatus in garnet growth during continuous prograde heating can cause resorption or a discontinuity in zoning profiles without calling upon multiple metamorphic "events" [this conclusion was also noted by Thompson *et al.* (1977)]; (3) a single explosive growth-event of garnet is predicted when cordierite first becomes stable, and (4) garnet is predicted to undergo reaction with cordierite during prograde growth as well as during retrograde re-equilibration. Whereas the specific details of zoning history predicted by the simulations are subject to several uncertainties in the model system, observations (2) and (3) are based on basic thermodynamic requirement *if* equilibrium in the matrix during growth of garnet is maintained.

The ratio of the mole fraction of a component in garnet (or any phase) to its mole fraction in another phase at equilibrium may not necessarily trend toward one with increasing temperature over a limited interval of temperature. Specifically, the ratio of Mn in garnet to that in the matrix cannot be relied upon as a measure of the relative temperature of nucleation without explicit calculation from thermodynamic data.

There are a great many assumptions included in the simulations described here. As solution models in exchange phases improve, and as a more precise knowledge is gained of the mechanisms and conditions of crystal growth in metamorphic environments, this type of simulation may continually be improved.

Acknowledgements

This work used the facilities of the University Computer Center, University of Arizona, and was supported by the Earth Sciences Section, National Science Foundation (NSF grant EAR–7904108). Robert Strauss contributed many days of programming effort. Thanks are due to J. Ganguly, R. Beane, C. T. Foster and L. S. Hollister for comments that resulted in improvement of previous versions.

References

Arkai, P., Nagy, G. & Panto, G. (1975): Types of composition zoning in the garnets of polymetamorphic rocks and their genetic significance. *Acta Geol. Acad. Sci. Hung.* **19**, 17-41.

Ashworth, J.R. (1975): Sillimanite zones of the Huntly – Portsoy area in the northeast Dalradian, Scotland. *Geol. Mag.* **112**, 113-136.

Atherton, M.P. (1968): The variation in garnet, biotite, and chlorite composition in medium grade pelitic rocks from the Dalradian, Scotland, with particular reference to the zonation in garnet. *Contr. Mineral. Petrology* **18**, 347-371.

Banno, S. & Kurata, H. (1972): Distribution of Ca in zoned garnet of low-grade pelitic schists. *J. Geol. Soc. Japan* **78**, 507-512.

Black, P.M. (1973): Mineralogy of New Caledonian metamorphic rocks. I. Garnets from the Ouégoa district. *Contr. Mineral. Petrology* **38**, 221-235.

BLACKBURN, W.H. (1969): Zoned and unzoned garnets from the Grenville gneisses around Gananoque, Ontario. *Can. Mineral.* **9**, 691-698.

BROWN, E.H. (1967): The greenschist facies in part of Eastern Otago, New Zealand. *Contr. Mineral. Petrology* **14**, 259-292.

BURNHAM, C.W., HOLLOWAY, J.R. & DAVIS, N.F. (1969): Thermodynamic properties of water to 1000°C and 10,000 bars. *Geol. Soc. Amer. Spec. Pap.* **132**.

CHEN, CHAO-HSIA (1975): A method of estimation of standard free energies of formation of silicate minerals at 298.15 K. *Amer. J. Sci.* **275**, 801-817.

CHINNER, G.A. (1960): Pelitic gneisses with varying ferrous/ferric ratios from Glen Clova, Angus, Scotland. *J. Petrology* **1**, 178-217.

——— (1962): Almandine in thermal aureoles. *J. Petrology* **3**, 316-340.

CLARK, L.D. (1961): Precambrian geology of the Norway Lake area. *In* Geology of Central Dickinson County, Michigan. *U. S. Geol. Surv. Prof. Pap.* **310**, 97-113.

CRAWFORD, M.L. (1966): Composition of plagioclase and associated minerals in some schists from Vermont, U.S.A., and South Westland, New Zealand, with inferences about the peristerite solvus. *Contr. Mineral. Petrology* **13**, 269-294.

CZAMANSKE, G.K. & MIHÁLIK, P. (1972): Oxidation during magmatic differentiation, Finnmarka complex, Oslo area, Norway. I. The opaque oxides. *J. Petrology* **13**, 493-509.

DALLMEYER, R.D. & DODD, R.T. (1971): Distribution and significance of cordierite in paragneisses of the Hudson Highlands, southeastern New York. *Contr. Mineral. Petrology* **33**, 289-308.

DE BÉTHUNE, S. (1976): Formation of metamorphic biotite by decarbonation. *Lithos* **9**, 309-318.

EDMUNDS, W.M. & ATHERTON, M.P. (1971): Polymetamorphic evolution of garnet in the Fanad aureole, Donegal, Eire. *Lithos* **4**, 147-161.

FERRY, J.M. (1976): Metamorphism of calcareous sediments in the Waterville–Vassalboro area, south-central Maine: mineral reactions and graphical analysis. *Amer. J. Sci.* **276**, 841-882.

——— & SPEAR, F.S. (1978): Experimental calibration of the partitioning of Fe and Mg between biotite and garnet. *Contr. Mineral. Petrology* **66**, 113-117.

FLETCHER, C.J.N. & GREENWOOD, H.J. (1979): Metamorphism and structure of Penfold Creek area, near Quesnel Lake, British Columbia. *J. Petrology* **20**, 743-794.

FOX, J.S. (1975): Three-dimensional isograds from the Lukmanier Pass, Switzerland, and their tectonic significance. *Geol. Mag.* **112**, 547-564.

FREY, M. (1978): Progressive low-grade metamorphism of a black shale formation, central Swiss Alps, with special reference to pyrophyllite and margarite bearing assemblages. *J. Petrology* **19**, 95-135.

GABLE, D.J. & SIMS, P.K. (1969): Geology and regional metamorphism of some high-grade cordierite gneisses, Front Range, Colorado. *Geol. Soc. Amer. Spec. Pap.* **128**.

GALWEY, A.K. & JONES, K.A. (1966): Crystal size frequency distribution of garnets in some analyzed metamorphic rocks from Mallaig, Inverness, Scotland. *Geol. Mag.* **103**, 143-152.

GANGULY, J. (1977): Compositional variables and chemical equilibrium in metamorphism. *In* Energetics of Geological Processes (S. Bhattacharji & S.K. Saxena, eds.), Springer-Verlag, New York.

GHENT, E. (1975): Temperature, pressure, and mixed-volatile equilibria attending metamorphism of staurolite–kyanite-bearing assemblages, Esplanade Range, British Columbia. *Geol. Soc. Amer. Bull.* **86**, 1654-1660.

GREEN, T.H. & RINGWOOD, A.E. (1968): Origin of garnet phenocrysts in calcalkaline rocks. *Contr. Mineral. Petrology* **18**, 163-174.

HARRIS, N.B.W. (1976): The significance of garnet and cordierite from the Sioux Lookout region of the English River gneiss belt, northern Ontario. *Contr. Mineral. Petrology* **55**, 91-104.

HARTE, B. & HENLEY, K.J. (1966): Occurrence of compositionally zoned almanditic garnets in regionally metamorphosed rocks. *Nature* **210**, 689-692.

HASELTON, H.T., JR. & WESTRUM, E.F., JR. (1979): Heat capacities (5–350 K) of synthetic pyrope, grossular, and $pyrope_{60}$ $grossular_{40}$. *Amer. Geophys. Union Trans.* **60**, 405 (abstr.).

HELGESON, H.C., DELANEY, J.M., NESBITT, H.W. & BIRD, D.K. (1978): Summary and critique of the thermodynamic properties of rock-forming minerals. *Amer. J. Sci.* **278-A**, 1-229.

HENRY, J. (1974): Garnet–cordierite gneisses near the Egersund–Ogna anorthositic intrusion, southwestern Norway. *Lithos* **7**, 207-216.

HESS, P.C. (1971): Prograde and retrograde equilibria in garnet–cordierite gneisses in south-central Massachusetts. *Contr. Mineral. Petrology* **30**, 177-195.

HOLLISTER, L.S. (1966): Garnet zoning: an interpretation based on the Rayleigh fractionation model. *Science* **154**, 1647-1651.

——— (1969): Contact metamorphism in the Kwoiek area of British Columbia: an end member of the metamorphic process. *Geol. Soc. Amer. Bull.* **80**, 2465-2494.

HOSCHEK, G. (1967): Untersuchungen zum Stabilitätsbereich von Chloritoid und Staurolith. *Contr. Mineral. Petrology* **14**, 123-162.

JONES, J.W. (1972): An almandine garnet isograd in the Rogers Pass area, British Columbia: the nature of the reaction and an estimation of the physical conditions during its formation. *Contr. Mineral. Petrology* **37**, 291-306.

JONES, K.A. & GALWEY, A.K. (1964): A study of possible factors concerning garnet formation in rocks from Ardara, Co. Donegal, Ireland. *Geol. Mag.* **101**, 76-93.

KAYS, M.A. & MEDARIS, L.G., JR. (1976): Petrology of the Hara Lake paragneisses, northeastern Saskatchewan, Canada. *Contr. Mineral. Petrology* **59**, 141-159.

KEPEZHINSKAS, K.B. (1973): Pressure variability during medium-temperature metamorphism of meta-pelites. *Lithos* **6**, 145-158.

KORIKOVSKIY, S.P., LAPUTINA, I. P. & GUSEVA, A.I. (1974): True almandine isograd in Precambrian metapelite of the Patom Mountains and stability of the garnet–chlorite paragenesis in kyanite complexes. *Dokl. Acad. Sci. USSR, Earth Sci. Sect.* **211**, 145-147.

KRAMM, U. (1976): The coticule rocks (spessartine quartzites) of the Venn–Stavelot massif, Ardennes, a volcanoclastic metasediment? *Contr. Mineral. Petrology* **56**, 135-155.

KRETZ, R. (1966): Grain-size distribution for certain metamorphic minerals in relation to nucleation and growth. *J. Geol.* **74**, 147-173.

——— (1973): Kinetics of the crystallization of garnet at two localities near Yellowknife. *Can. Mineral.* **12**, 1-20.

KURATA, H. & BANNO, S. (1974): Low-grade progressive metamorphism of pelitic schists of the Sazare area, Sanbagawa metamorphic terrain in central Sikoku, Japan. *J. Petrology* **15**, 361-382.

LOOMIS, T.P. (1972): Contact metamorphism of pelitic rock by the Ronda ultramafic intrusion, southern Spain. *Geol. Soc. Amer. Bull.* **83**, 2449-2473.

——— (1982): Numerical simulation of disequilibrium growth processes of garnet in chlorite-bearing, aluminous pelitic rocks. *Can. Mineral.* **20**, 411-423.

MCATEER, C. (1976): Formation of garnets in a rock from Mallaig. *Contr. Mineral. Petrology* **55**, 293-301.

MCCALLISTER, R.H., BOCTOR, N.Z. & HINZE, W.J. (1978): Petrology of the spilitic rocks from the Michigan Basin deep drill hole. *J. Geophys. Res.* **83**, 5825-5831.

MIYASHIRO, A. & SHIDO, F. (1973): Progressive compositional change of garnet in metapelite. *Lithos* **6**, 13-20.

NAVARRO, E. & BLACKBURN, W.H. (1974): Investigations in the basement rocks of Gunnison County, Colorado: the metasedimentary rocks. *Neues Jahrb. Mineral. Abh.* **122**, 246-267.

NEWTON, R.C., THOMPSON, A.B. & KRUPKA, K.M. (1977): Heat capacity of synthetic $Mg_3Al_2Si_3O_{12}$ from 350 to 1000 K and the entropy of pyrope. *Amer. Geophys. Union Trans.* **58**, 523 (abstr.).

OKRUSCH, M. (1971): Garnet–cordierite–biotite equilibria in the Steinach aureole, Bavaria. *Contr. Mineral. Petrology* **32**, 1-23.

PETTIJOHN, F.J. (1949): *Sedimentary Rocks.* Harper and Row, New York.

ROBIE, R.A., HEMINGWAY, B.S. & FISHER, J.R. (1978): Thermodynamic properties of minerals and related substances at 298.15 K and 1 bar (10^5 pascals) pressure and at higher temperatures. *U.S. Geol. Surv. Bull.* **1452**.

SAXENA, E.K. (1969): Silicate solid solutions and geothermometry. 4. Statistical study of chemical data on garnets and clinopyroxene. *Contr. Mineral. Petrology* **23**, 140-156.

SCHMID, R. & WOOD, B.J. (1976): Phase relationships in granulitic metapelites from the Ivrea–Verbano zone (northern Italy). *Contr. Mineral. Petrology* **54**, 255-279.

SEIDEL, E., OKRUSCH, M., KREUZER, H. RASCHKA, H. & HARRE, W. (1976): Eoalpine metamorphism in the uppermost unit of the Cretan nappe system – petrology and geochronology. 1. The Léndas area (Asteroúsia Mountains). *Contr. Mineral. Petrology* **57**, 259-275.

SEKINO, H. NAGASHIMA, K. & HARADA, K. (1973): Manganese bearing hydromuscovite from Tanakami-yama pegmatite, Shiga Prefecture, Japan. *Neues Jahrb. Mineral. Monatsh.*, 189-192.

STEPHENSON, N.C.N. (1979): Coexisting garnets and biotites from Precambrian gneisses of the south coast of Western Australia. *Lithos* **12**, 73-87.

THOMPSON, A.B. (1976): Mineral reactions in pelitic rocks. II. Calculation of some P–T–*X* (Fe–Mg) phase relations. *Amer. J. Sci.* **276**, 425-454.

——— TRACY, R.J., LYTTLE, P.T. & THOMPSON, J.B., JR. (1977): Prograde reaction histories deduced from compositional zonation and mineral inclusions in garnet from the Gassetts schist, Vermont. *Amer. J. Sci.* **277**, 1152-1167.

TRACY, R.J., ROBINSON, P. & THOMPSON, A.B. (1976): Garnet composition and zoning in the determination of temperature and pressure of metamorphism, central Massachusetts. *Amer. Mineral.* **61**, 762-775.

WEAVER, C.E. & BECK, K.C. (1971): Clay water diagenesis during burial: how mud becomes gneiss. *Geol. Soc. Amer. Spec. Pap.* **134**.

WINKLER, H.G.F. (1974): *Petrogenesis of Metamorphic Rocks.* Springer-Verlag, New York.

WOODSWORTH, G.J. (1977): Homogenization of zoned garnets from pelitic schists. *Can. Mineral.* **15**, 230-242.

YARDLEY, B.W.D. (1977): An empirical study of diffusion in garnet. *Amer. Mineral.* **62**, 793-800.

Received February 1982, revised manuscript accepted April 1982.